Optimizing imperfect cloaks to perfection

Liang-Wu Cai
Department of Mechanical and Nuclear Engineering, Kansas State University, Manhattan, Kansas 66506

(Received 30 November 2011; revised 22 February 2012; accepted 19 March 2012)

Transformation optics has been an essential tool for designing cloaking devices for electromagnetic and acoustic waves. All these designs have one requirement in common: material singularity. At the interface between the cloak and the cloaked region, some material properties have to approach infinity, while some others approach zero. This paper attempts to answer a central question in physically realizing such cloaks: is material singularity a requirement for perfect cloaking? This paper demonstrates that, through optimization, perfect cloaking can be achieved using a layered cloak construction without material singularity. Two examples are used for this demonstration. In one example, the initial design is based on the Cummer–Schurig prescription for acoustic cloaking that requires mass-anisotropic material. Another example uses the two isotropic layers to achieve the equivalent mass-anisotropy for each anisotropic layer. During the optimization processes, only material properties of cloaks' constituent layers are adjusted while the geometries remain unchanged. In both examples, the normalized total scattering cross section can be reduced to 0.002 (0.2%) or lower in numerical computations. The capabilities and other characteristics of the optimization in other tasks such as cloaking penetrable objects and isolating strong resonance in such objects are also explored.
 [http://dx.doi.org/10.1121/1.4744979]

PACS number(s): 43.20.El, 43.20.Bi [ANN] Pages: 2923–2931

I. INTRODUCTION

In the past few years, the topic of cloaking has attracted significant research interest since the demonstration of cloaking for microwaves.[1] The design was based on transformation optics.[2,3] In essence, a simply connected region is transformed into a region with an opening in its interior, a multi-connected region. If this new space is the physical space, anything inside the opening would be invisible and hence "cloaked." The transformation dictates the material properties required for the cloak, the transformed region. Since then, many cloaking designs, for both electromagnetic and acoustic waves, have been proposed. In general, the required material properties are rather "otherworldly." The collective efforts by the research community to design and characterize man-made materials that can effectively behave the way as prescribed in various designs have led to the emergence of a new area of research called "metamaterials."

This paper is focused on acoustic cloaking. Among many proposed designs for acoustic cloaking, the most important one, the canonical design, was proposed by Cummer and Schurig.[4] The Cummer–Schurig design of a circular acoustic cloak requires a mass-anisotropic material whose properties vary along the radial direction in the following prescribed manner:

$$\frac{\rho_r}{\rho_0} = \frac{r}{r-a}, \tag{1}$$

$$\frac{\rho_\theta}{\rho_0} = \frac{r-a}{r}, \tag{2}$$

$$\frac{K}{K_0} = \left(\frac{b-a}{b}\right)^2 \frac{r}{r-a}, \tag{3}$$

where parameters with subscript 0 belong to the host medium; ρ and K are the mass density and bulk modulus, respectively; and a and b are the inner and outer radii of the cloak, respectively. The mass anisotropy is assumed to be orthotropic, having a diagonal mass density tensor when written in the polar coordinate system (r, θ) that originates at the center of the cloaked region.

There are two significant challenges in this prescription when one attempts to physically realize such a cloak. The first is the mass anisotropy, which is not a commonly observed feature in any material that can be found in the natural world. The second challenge is the material singularity: at the interface between the cloak and the cloaked region, $r = a$, the prescription requires $\rho_r \to \infty$ and $K \to \infty$, while $\rho_\theta \to 0$.

The mass anisotropy can probably be addressed by the idea of using two isotropic layers to mimic an anisotropic layer.[5,6] The effective mass-anisotropic material properties obtained from homogenizing two isotropic layers, denoted as layers A and B, are

$$\rho_r = \frac{1}{1+\eta}(\rho_A + \eta\rho_B), \tag{4}$$

$$\frac{1}{\rho_\theta} = \frac{1}{1+\eta}\left(\frac{1}{\rho_A} + \frac{\eta}{\rho_B}\right), \tag{5}$$

$$\frac{1}{K} = \frac{1}{1+\eta}\left(\frac{1}{K_A} + \frac{\eta}{K_B}\right), \tag{6}$$

where η is the thickness ratio of layer B to layer A. An in-depth analysis of this analogy has recently been given by the author and his colleague.[7] With the possibility of such, the research community appears to have reached a consensus

that a feasible approach is to use a layered structure to approximate the continuously varying properties of the Cummer–Schurig prescription. Inevitably, such an approximation, in conjunction with the physical unachievability of material singularity, would sacrifice the effects of cloaking, leading to an imperfect cloak.

Recently, a non-singular cloak design based on the transformation optics has been proposed:[8] Instead of a mathematical point, a tiny opening is transformed into a sizable opening in the physical space. However, the resulting cloak is imperfect, and yet it still requires that one of the mass density components approach zero, which might be viewed as another form of singularity.

In this author's opinion, such imperfection should only be viewed with regards to precisely following the prescription of transformation optics. In regard to cloaking effects, a more philosophical question should be asked first: Is the material singularity a requirement for perfect cloaking? Or, is it just an inconvenient artifact due to the use of transformation optics? This paper attempts to bring an optimistic answer to this question.

In this paper, various optimization schemes are used to fine tune the parameters in layered cloaks, while using the Cummer–Schurig prescription as initial designs. It is demonstrated that, numerically and from an engineering perspective, material singularity is not a requirement. With finite values in acoustic properties and a finite number of uniform layers, perfect cloaking can be achieved.

This paper is organized as follows. Section II describes the details of the optimization process. Section III demonstrates the perfect cloaking without material singularity with two examples, both based on the Cummer–Schurig prescription, for cloaking a rigid cylinder, as intended in the ideal Cummer–Schurig cloak. Section IV explores the behaviors of the optimized cloaks when they are used to cloak penetrable objects, and what object-specific optimizations are capable of. Section V offers a brief discussion on some characteristics of the optimization processes. The paper is concluded in Sec. VI.

II. OPTIMIZATION PROCEDURES

A solution to a problem can be optimized if there are alternative solutions and there is a quantitative way of telling which is the better solution. It is formulated into an optimization problem by introducing the *objective function* that quantifies the goodness of a solution, and a set of *optimization variables* that can be varied to arrive at different solutions. Then, this optimization process is concerned with finding the minimum of the objective function within the allowable range of the optimization variables.

A. The objective function

For cloak designs, there is a well-defined and widely used scalar quantity called the "total scattering cross section" that naturally fits as the objective function to minimize. The total scattering cross section is defined as the total energy scattered by a scatterer over a closed surface enclosing the scatterer and normalized by the energy flux of the planar incident wave. The total scattering cross section is a positive-semidefinite parameter, which vanishes only when the scatterer is completely invisible, or being perfectly cloaked. It has the unit of an area; and in the high frequency limit, it approaches the geometric cross-sectional area of the scatterer. For this reason, the total scattering cross-section is often further normalized by its geometric cross-sectional area, which, for the case of a cylindrical scatterer, is the diameter of the scatterer.

Scattering problems are often solved by using modal expansions in which different waves are expanded into different modes. The T-matrix is the matrix that relates the wave expansion coefficients of the scattered wave to those of the incident wave. In essence, it represents the complete solution to a single scattering problem. For an axisymmetric scatterer, its T-matrix is diagonal; and the expression for its normalized scattering cross section can be written as

$$\tilde{\sigma} = \frac{2}{\pi ka} \sum_{n=-\infty}^{\infty} |[T]_n|^2, \tag{7}$$

where $[T]_n$ is the entry of its T-matrix at the n-th column and the n-th row, and the total scattering cross section has been normalized by the diameter of the cloaked region, $2a$.

A computational procedure for evaluating the T-matrix and other scattering characteristics for multi-layered two-dimensional scatterers has been developed by the author and his colleagues.[9,10] A similar scheme for three-dimensional scatterers has also been developed recently.[11] This is an iterative scheme for analyzing a scatterer comprised of an arbitrary number of concentric layers, yielding analytically exact solutions for the T-matrix. Combined with the solutions to scattering problems in mass-anisotropic materials,[12] this scheme has allowed the author and his colleague to analyze the original Cummer–Schurig cloak,[12] by approximating the continuously varying cloak as a multi-layered cloak, with each layer being made of an uniform anisotropic material.

B. Optimization schemes

Broadly speaking, there are three classes of well-established and widely used optimization schemes. They require the capabilities of evaluating the zeroth- (the function itself), the first-, and the second-derivatives, respectively, of the objective function. The direct search method, gradient method, and quasi-Newton's method are the representative examples of these classes. The first class would be too slow for cloak optimization since each cloak design involves a large number of parameters, each of which has a cast range of material properties to choose from. Having only the numerical tool to evaluate the objective function, the evaluation of the second derivative is unreliable. Thus, the gradient-based method is the most suitable choice.

The classic gradient-based method is the so-called "steepest descent method." For a multivariable function, the negative of the gradient at a point points to the direction of the steepest descent. Heuristically this would be the best direction to march toward minimizing the objective function. The search marches in the following manner: at the n-th step in the optimization process, the next optimal parameter set is determined by

$$\boldsymbol{x}_{n+1} = \boldsymbol{x}_n - h_n \nabla \tilde{\sigma}|_{\boldsymbol{x}_n}, \tag{8}$$

where h_n is the step size, and $\boldsymbol{x}$ denotes the set of parameters (optimization variables) that affects the objective function. Typically h_n is determined at each step such that it reaches the minimum in that particular direction. In determining the step size, one-dimensional optimization schemes can be used.

A variation to this is the so-called "conjugate gradient method," in which the search direction is modified, to avoid the zigzagness of the search path. The modified direction, denoted as $\boldsymbol{d}_n$, is expressible as

$$\boldsymbol{d}_n = -\nabla \tilde{\sigma}|_{\boldsymbol{x}_n} + \beta_n \boldsymbol{d}_{n-1} \tag{9}$$

and the new parameter set is

$$\boldsymbol{x}_{n+1} = \boldsymbol{x}_n + h_n \boldsymbol{d}_n. \tag{10}$$

There are different approaches to correcting the search direction for general nonlinear objective functions, giving different expressions for β_n. The readers are referred to many textbooks on nonlinear optimization, such as Ref. 13, for specific varieties. Specifically, the formulas of Hestenes–Stiefel, Fletcher–Reeves, and Polak–Ribiére have all been implemented.

In the optimization schemes used in this paper, the step size h_n is determined in the following manner. First, a maximum allowable step size $h_{\max}$ is defined *a priori*. This is a safeguard to avoid the parameters being changed too drastically within a step. Within a search step, $h_{\max}$ is taken as the initial trial step size and the corresponding trial parameter set is denoted as $\boldsymbol{x}_{n+1}^{\text{trail}}$. If $\tilde{\sigma}(\boldsymbol{x}_{n+1}^{\text{trail}}) < \tilde{\sigma}(\boldsymbol{x}_n)$, $h_{\max}$ is not large enough to bring the search to the minimum in this direction. But it is used as the step size since it is the maximum allowable size. Otherwise, the step size is reduced by a certain percentage set *a priori*, which in turn defines a new trial parameter set. This process is repeated until the condition $\tilde{\sigma}(\boldsymbol{x}_{n+1}^{\text{trail}}) < \tilde{\sigma}(\boldsymbol{x}_n)$ is reached.

By this time, if $h_{\max}$ has not been taken as the step size, at least three parameter sets have been identified: the current parameter set $\boldsymbol{x}_n$, the latest trial parameter set denoted as x_1^{trail}, and the previous (next to the last) trial parameter set denoted as $\boldsymbol{x}_2^{\text{trail}}$. They correspond to three points on the $h - \tilde{\sigma}$ plane along the search direction, with abscissas at 0, h_1^{trail}, and h_2^{trail}. They satisfy the following relations: $0 < h_1^{\text{trail}} < h_2^{\text{trail}}$ and $\tilde{\sigma}(\boldsymbol{x}_1^{\text{trail}}) < \tilde{\sigma}(\boldsymbol{x}_n) < \tilde{\sigma}(\boldsymbol{x}_2^{\text{trail}})$. These three points can be fitted with a parabolic curve, a process known as the "inverse parabolic fitting."[14] The fitted curve has its minimum within the range $(0, h_2^{\text{trail}})$, located at

$$h_n = h_1^{\text{trail}} - \frac{1}{2}\frac{(h_1^{\text{trail}})^2[\tilde{\sigma}(x_1^{\text{trail}}) - \tilde{\sigma}(x_2^{\text{trail}})] - (h_1^{\text{trail}} - h_2^{\text{trail}})^2[\tilde{\sigma}(x_1^{\text{trail}}) - \tilde{\sigma}(x_n)]}{h_1^{\text{trail}}[\tilde{\sigma}(x_1^{\text{trail}}) - \tilde{\sigma}(x_2^{\text{trail}})] - (h_1^{\text{trail}} - h_2^{\text{trail}})[\tilde{\sigma}(x_1^{\text{trail}}) - \tilde{\sigma}(x_n)]}. \tag{11}$$

If desired, the inverse parabolic fitting can be repeated to refined the parameter set that would minimize the objective function. Since this is only an intermediate step in the optimization process, precisely locating the minimal point in a trial direction is not crucial. In the optimization schemes used in this paper, the inverse parabolic fitting is only performed once.

The optimization is considered converged if the objective function evaluated with the new parameter set falls below the target value. On the other hand, if the search in the gradient or conjugate gradient direction requires a step size that is extremely small, the optimization is considered stalled.

In this paper, optimizations are run unconstrained.

III. PERFECT CLOAKING WITHOUT MATERIAL SINGULARITY

In this section, examples are used to demonstrate that perfect cloaking with a finite number of uniform layers without material singularity is possible. In the numerical optimization runs, the criterion for the convergence is

$$\tilde{\sigma} < 0.002 \ (0.2\%). \tag{12}$$

Two designs are considered.

A. Cloak with anisotropic layers

The first cloak to be optimized consists of five anisotropic layers of equal thickness, based on the Cummer–

TABLE I. Material properties for cloak comprised of five anisotropic layers, including both initial and optimized designs.

		ρ_r/ρ_0			ρ_θ/ρ_0			c_r/c_0			K/K_0		
Layer	r_i	Initial	Optimized	Change (%)	Initial	Optimized	Change (%)	Initial	Optimized	Change (%)	Initial	Optimized	Change (%)
1	1.36	3.7778	3.7746	−0.08365	0.26471	0.27256	2.964	0.28571	0.28383	−0.6603	0.30839	0.30408	−1.399
2	1.28	4.5714	4.5681	−0.07175	0.21875	0.22058	0.8366	0.28571	0.29207	2.225	0.37318	0.38969	4.426
3	1.20	6.0000	5.9960	−0.06717	0.16667	0.17454	4.724	0.28571	0.28700	0.4501	0.48980	0.49388	0.8344
4	1.12	9.3337	9.3115	−0.2374	0.10714	0.11424	6.625	0.28571	0.28491	−0.2831	0.76193	0.75582	−0.8015
5	1.04	26.000	26.011	0.04269	0.038463	0.038393	−1.812	0.28571	0.34365	20.28	2.1224	3.0718	44.73

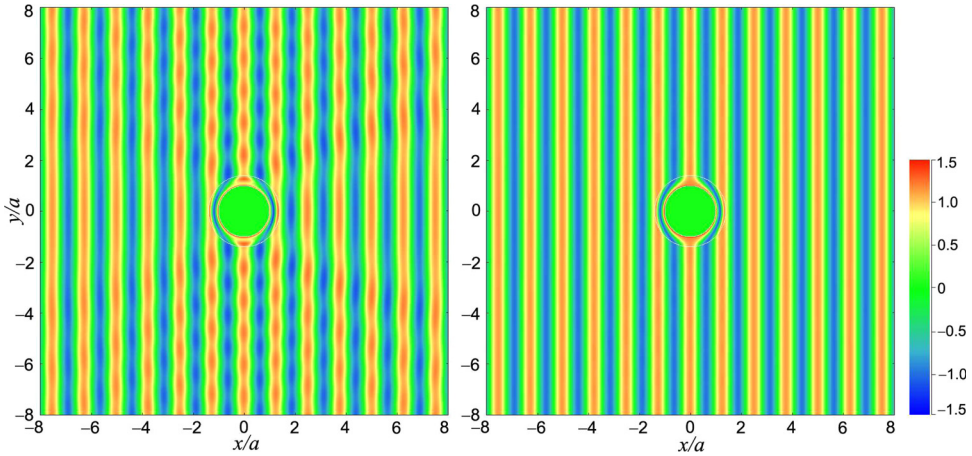

FIG. 1. (Color online) Snap shots of total wave field when a planar incident wave of frequency $ka = 5$ impinges onto a cloaked rigid cylinder. The cloak is comprised of five anisotropic layers based on the Cummer–Schurig prescription. Left: initial design. Right: optimized cloak.

Schurig prescription. The cloak thickness is 40% of the radius of the cloaked region; that is, $b = 1.4a$. Each layer is assumed to be uniform, having material properties as prescribed by Eqs. (1)–(3) at each layer's median radius. The host is assumed to be water, of a mass density of 1000 kg/m^3, and a sound speed of 1350 m/s. The cloaked region is assumed to be rigid.

The optimization is focused on the material properties of individual layers. The geometry, the number of layers, and the properties of the cloaked region are not altered during the optimization. The computation of the normalized total scattering cross section uses the radial and circumferential mass densities and the radial sound speed. The bulk modulii and the circumferential sound speeds are not used. Thus, the optimization variables include only the mass densities and the radial sound speeds of individual layers, totaling 15 parameters. During the optimization, the scattering cross section is evaluated at $ka = 5$. The optimization runs with different schemes converge typically within 8–10 iterations, from an initial normalized total scattering cross section of $\tilde{\sigma} = 0.21816$. They generally converge rapidly, with every step making a significant reduction in the total scattering cross section.

The material properties for the initial and the optimized designs are listed in Table I. In Table I, the r_i column lists the median radius for each layer where Eqs. (1)–(3) are evaluated and taken as the layer's uniform properties. The "change" columns list the percentage changes of material properties in the optimized design from the initial design. It can be seen that the changes are rather mild, with the largest being 20% increase in radial sound speed for the inner-most layer: from 385.7 to 463.9 m/s.

A snapshot of the pressure field (the real part of the complex amplitude of acoustic pressure) for the optimized design is compared with that of the initial design in Fig. 1, when an planar incident wave of frequency $ka = 5$, the frequency at which the optimization is run, impinges onto the cloaked cylinder. The normalized total scattering cross section of both designs are compared in Fig. 2 over the frequency range from $ka = 0$ to 6.

It can be observed from Figs. 1 and 2 that, although the initial design already has excellent cloaking capability, the optimization process is able to reduce the total scattering cross section further by two orders of magnitude, to a level that can be justifiably called perfect cloaking in any practical sense. Although the Cummer–Schurig design is frequency independent, the total scattering cross section in general is frequency dependent. And yet, the lack of mass singularity certainly adds a degree of frequency dependency. The initial design exhibits its frequency dependency as early as $ka = 2$, as indicated by the significant rate of increase in the scattering cross section. The optimized design defers this occurrence until $ka = 5$, the frequency at which the optimization was run.

B. Cloak with isotropic layers

The second cloak to be optimized is also based on the five anisotropic layers as prescribed by the Cummer–Schurig design in Eqs. (1)–(3), but each anisotropic layer is then replaced by a pair of isotropic layers, using Eqs. (4)–(6). In other words, it consists of ten isotropic layers. The overall thickness of the cloak is 20% of the cloaked region; that is, $b = 1.2a$.

Note that Eqs. (4)–(6) are not sufficient for determining all the parameters of both isotropic layers. One additional condition is needed.[7] Assuming that the two layers are of equal thickness, that is, $\eta = 1$, then, Eqs. (4) and (5) give

$$\rho_{A,B} = \rho_r \pm \sqrt{\rho_r(\rho_r - \rho_\theta)}. \tag{13}$$

Assuming that the bulk modulii of the two isotropic layers are proportional to their mass densities, that is $K_A/K_B = \rho_A/\rho_B$, then Eq. (6) gives

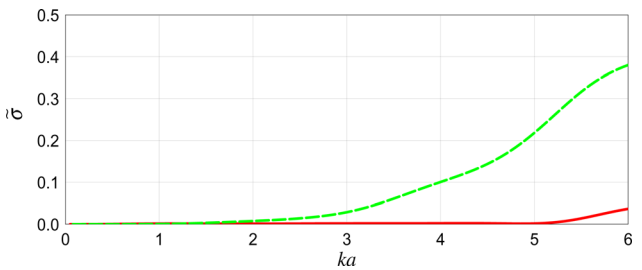

FIG. 2. (Color online) Normalized total scattering cross section of the cloak comprised of five anisotropic layers. Solid: optimized cloak. Dashed: initial design.

TABLE II. Material properties for cloak comprised of ten isotropic layers, including both initial and optimized designs.

		ρ/ρ_0			c/c_0			K/K_0		
Layer	r_i	Initial	Optimized	Change (%)	Initial	Optimized	Change (%)	Initial	Optimized	Change (%)
1	1.18	0.076720	0.10341	34.79	1.0926	0.98023	−10.28	0.091585	0.099362	8.492
2	1.18	13.034	13.075	0.3084	1.0926	1.0923	−0.03119	15.560	15.598	0.2459
3	1.14	0.061637	0.062430	1.284	1.3571	1.3089	−3.556	0.11353	0.10695	−5.791
4	1.14	16.224	16.228	0.0240	1.3571	1.3570	−0.01037	29.882	29.883	0.003294
5	1.10	0.045549	0.028911	−36.53	1.8333	1.7547	−4.287	0.15310	0.089019	−41.85
6	1.10	21.955	21.957	0.0100	1.8333	1.8333	−0.004040	73.792	73.793	0.001939
7	1.06	0.028325	0.023216	−18.04	2.9444	2.9173	−0.9225	0.24557	0.19758	−19.54
8	1.06	35.305	35.308	0.009347	2.9444	2.9444	−0.0002516	306.09	306.11	0.008844
9	1.02	0.0098050	0.0099610	1.588	8.5000	8.4915	−0.06885	0.70840	0.71866	1.449
10	1.02	101.99	101.99	0	8.5000	8.5000	0	7368.8	7368.8	0

$$K_A = \frac{K}{2}\left(1+\frac{\rho_A}{\rho_B}\right), \quad K_B = \frac{K}{2}\left(1+\frac{\rho_B}{\rho_A}\right). \tag{14}$$

This way, the two layers have the same sound speed, ensuring the wave numbers in both layers being in the same order.

In evaluating the total scattering cross section, the mass densities and sound speeds of individual layers are used. Bulk modulii are not used. Thus the optimization variables include the mass densities and sound speeds of individual layers, 20 in total. The optimization was run at $ka = 3$. Compared with the anisotropic cloak, the optimization runs for this cloak converge much slower after the initial few iterations, and generally taking 40–50 iterations. The initial normalized scattering cross section is $\tilde{\sigma} = 0.50201$, which is approximately 2.3 times of the first example. But this difference is diminished after the first iteration.

The material properties of both the initial design and the optimized design are listed in Table II. The r_i column in Table II lists the median radius at which Eqs. (1)–(3) are evaluated for the corresponding five-anisotropic layer design. For this reason, each pair has the same r_i value, which is also the radius of the interface of the two layers. The isotropic layer pairs are arranged such that the lighter layer is located outside (with an odd layer number), and the heavier layer is inside (with an even layer number). It is observed that all the large percentage changes in the material properties listed in Table II belong to the lighter layers, and the changes in absolute values are rather small.

The distributions of amplitude of the total acoustic pressure surrounding the cloaked rigid cylinder when a planar incident wave of frequency $ka = 3$, the frequency at which the optimization is run, impinges onto the cloaked cylinder are shown in Fig. 3 for both initial and the optimized designs. The normalized total scattering cross sections of both the initial design and the optimized design are compared in Fig. 4 over the frequency range from $ka = 0$ to 6.

From Fig. 4, a strong frequency dependency is observed in both initial and optimized designs. The main reason for such frequency dependency is that the equivalence between a pair of isotropic layers and a single anisotropic layer is valid only at low frequencies, as the first order approximation.[7] As the frequency increases, the equivalence deteriorates, and the frequency dependency emerges. Figure 4 suggests that this likely starts at a frequency as low as $ka \approx 1$, as indicated by the significant rate of increase in the scattering cross section of the initial design. However, the optimization is able to maintain excellent cloaking effects over a much wider frequency range, until $ka \approx 3$, the frequency at which the optimization was run. As with the anisotropic cloak, the frequency at which the optimization was run appears to have set the upper frequency limit for cloaking effectiveness.

IV. CLOAKING PENETRABLE OBJECTS

Cloaking penetrable objects is more challenging than cloaking a rigid object, because penetrable objects can

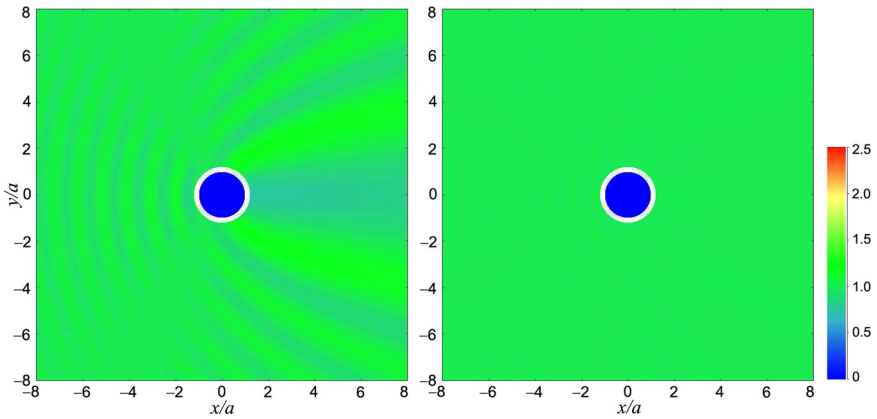

FIG. 3. (Color online) Distribution of amplitudes of total acoustic pressure when a planar incident wave of frequency $ka = 3$ impinges onto a cloaked rigid cylinder. The cloak is comprised of ten isotropic layers. Left: initial design. Right: optimized cloak.

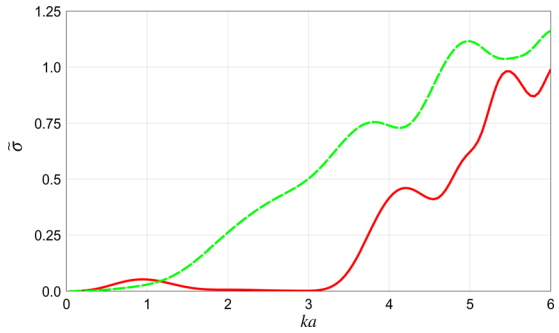

FIG. 4. (Color online) Normalized total scattering cross section of the cloak comprised of ten isotropic layers. Solid: optimized cloak. Dashed: initial design.

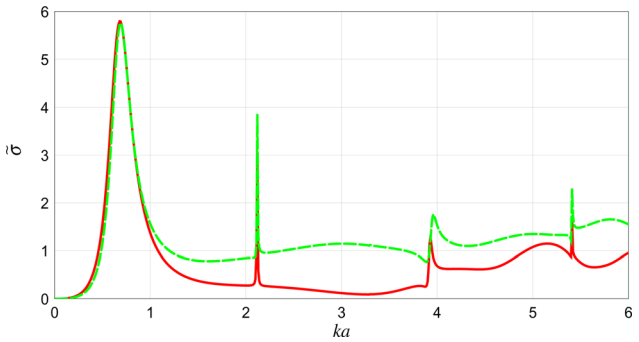

FIG. 6. (Color online) Normalized total scattering cross section of the cloak comprised of ten isotropic layers when it is used to cloak a water column. Solid: optimized for cloaking a rigid cylinder. Dashed: initial design.

resonate at certain frequencies. The ideal Cummer–Schurig cloak, even with material singularity, is penetrated at resonant frequencies.[12] Therefore, it would be interesting to observe how the optimized cloaks behave when they are used to cloak a penetrable object, and whether the optimization can be utilized to alleviate the problems that may arise.

First, the behaviors of the two cloaks optimized for rigid cylinders are observed when the rigid cylinder is replaced by a penetrable object. In this case, the cloaked region is filled with water, the same as the host medium. The normalized total scattering cross section of both cloaks are shown in Figs. 5 and 6, in comparison with their respective initial designs.

It can be observed that, when the core is replaced by the water column, there is a very strong resonance at $ka \approx 0.7$, and followed by a few weaker ones. Note that the two cloaks have different thicknesses and different material properties, and yet two of the resonances occurred at the same frequency in both cases (at $ka \approx 0.7$ and 3.9), and two other resonances shifted slightly, to lower frequencies for the thinner isotropic cloak.

For the anisotropic cloaks, the overall performances of the initial and the optimized designs are very similar. The optimized cloak performs slightly better. For the isotropic cloaks, the optimized cloak performs significantly better than the initial design, especially in the frequency range between the first the third resonances. This means that the optimization has indeed made both cloaks perform better even when the object to be cloaked is changed from what they are optimized for. For the two initial designs, the anisotropic cloak yields significantly smaller scattering cross section than the isotropic cloak. But, for the two optimized cloaks, the isotropic cloak performs better.

Second, the same optimization process is run to specifically optimize for cloaking the water column, $ka = 3$. The initial normalized scattering cross section for the two cloaks are $\tilde{\sigma} = 0.40612$ for the anisotropic cloak and 1.14615 for the isotropic cloak. The optimization takes 184 iterations for the anisotropic cloak and 34 iterations for the isotropic cloak to converge, just opposite to the case when cloaking a rigid cylinder. It is also worthy of noting that the optimization for the anisotropic cloak at $ka = 4$ and 5 stalled in just a few iterations, although the reduction in the scattering cross section might be significant, it could not reach the goal value.

The normalized total scattering cross section of both water-column-optimized cloaks are shown in Figs. 7 and 8 in comparison with their respective initial designs. The optimization does not alter the strong resonance noticeably, but it generally reduces the scattering cross section over a broad frequency range between the first and third resonances. The isotropic cloak performs better after the optimization. However, for the case of anisotropic cloak, it seems that the optimized design has introduced its own resonance at $ka \approx 6$.

Third, the same optimization process is run at the strongest resonance frequency $ka = 0.7$ for both cloaks. The initial normalized scattering cross section for the two cloaks are $\tilde{\sigma} = 5.72531$ for the anisotropic cloak and 5.70708 for

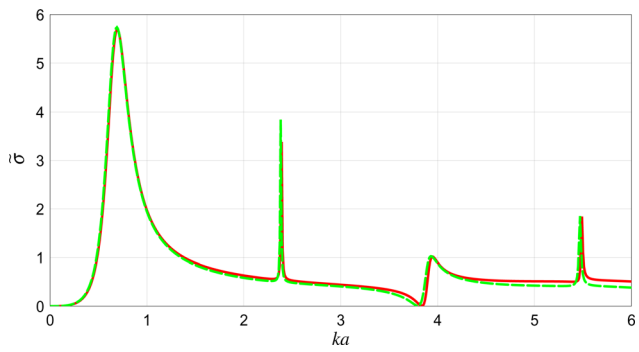

FIG. 5. (Color online) Normalized total scattering cross section of the cloak comprised of five anisotropic layers when it is used to cloak a water column. Solid: optimized for cloaking a rigid cylinder. Dashed: initial design.

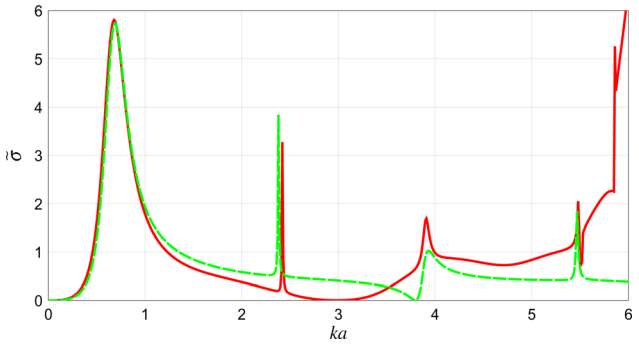

FIG. 7. (Color online) Normalized total scattering cross section of the cloak comprised of five anisotropic layers when it is used to cloak a water column. Solid: optimized for cloaking water column at $ka = 3$. Dashed: initial design.

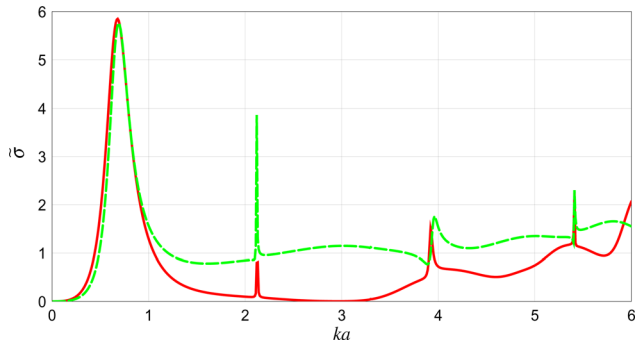

FIG. 8. (Color online) Normalized total scattering cross section of the cloak comprised of ten isotropic layers when it is used to cloak a water column. Solid: optimized for cloaking water column at $ka = 3$. Dashed: initial design.

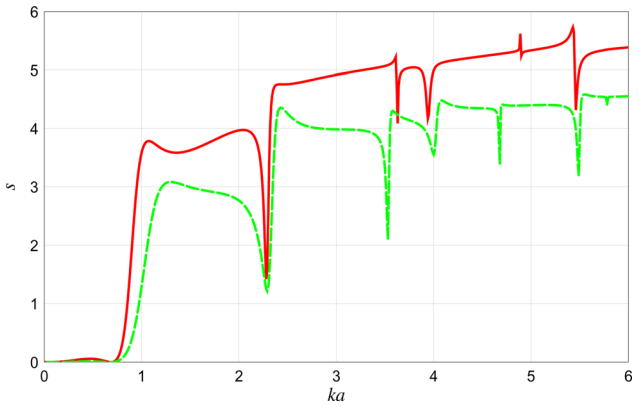

FIG. 9. (Color online) Normalized total scattering cross section of two cloaks specifically optimized for cloaking water column at $ka = 0.7$ where the initial designs of both cloaks show strong resonance. Solid: cloak comprised of five anisotropic layers. Dashed: cloak comprised of ten isotropic layers. Note the cloaking capability remains in the frequency range $ka < 0.7$ for both cloaks.

the isotropic cloak. The optimization processes appear to be much more "strenuous," as the total scattering cross sections of the initial designs are one order of magnitude larger than the previous cases, and more than three orders of magnitude larger than the target value. The optimization converges after 531 iterations for the anisotropic cloak and 4636 iterations for the isotropic cloak, with the maximum allowable step size being taken in most of these steps. These large numbers of iteration steps mean that material properties have deviated significantly from the initial designs. Figure 9 shows the normalized total scattering cross section of both designs optimized specifically for suppressing the resonance at $ka = 0.7$.

Figure 9 shows a general loss of the cloaking capability of both cloaks. This is expected, due to the large numbers of optimization iterations. However, the following two important observations from this experiment can be made. The first is that the results demonstrate the remarkable power of optimization for achieving perfect cloaking at the strongest resonant frequency. Of course, this is achieved at a cost. The second is that the cloaking capabilities of both cloaks are essentially maintained for frequencies below $ka = 0.7$, yet again, the frequency at which the optimization is run. Of the two optimized cloaks, the isotropic cloak performs better throughout the entire frequency range.

It is also of interest to observe what happens to the resonance with the optimized cloaks. Figure 10 shows the snap shots of the pressure field in the vicinity of the anisotropic cloak due to an impinging planar incident wave of frequency $ka = 0.7$. It can be seen that the resonance remains, as indicated by the large amplitude inside the water column. However, the optimized cloak is capable of completely confining the resonance to within the water column without leaving any trace to the exterior. Figure 11 show the amplitude distribution of the total acoustic pressure near the water column cloaked by the isotropic cloak due to an impinging planar incident wave of frequency $ka = 0.7$. This optimized cloak is also capable of completely confining the resonance inside the water column without leaving a trace to the exterior. In view of suppressing and isolating the resonance, both optimized cloaks work extremely well.

V. DISCUSSIONS

Having observed a few cases of perfect cloaking, at least when cloaking a rigid cylinder, being achieved without material singularity, one question immediately arises: at what price? The answer is that such a perfect cloaking is effective only limited to a certain frequency range.

The original design as proposed by Cummer and Schurig, requiring mass-anisotropy and material singularity, is a frequency-independent design.[12] This characteristic is largely inherited when using anisotropic layers, optimized or not, making such cloaks weakly frequency dependent. The

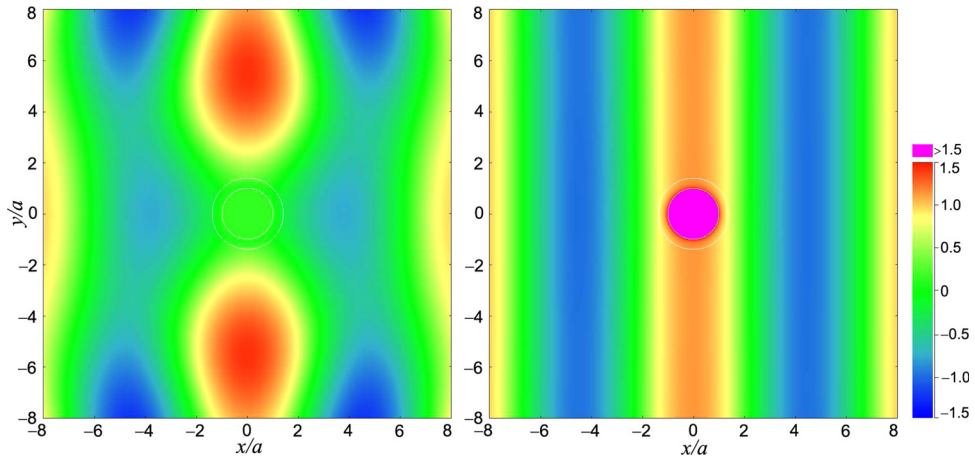

FIG. 10. (Color online) Snap shot of acoustic pressure field when a planar incident wave of frequency $ka = 0.7$ impinges onto a cloaked resonating water column. The cloak is comprised of five anisotropic layers. Left: initial design. Right: cloak specifically optimized for cloaking at the resonant frequency.

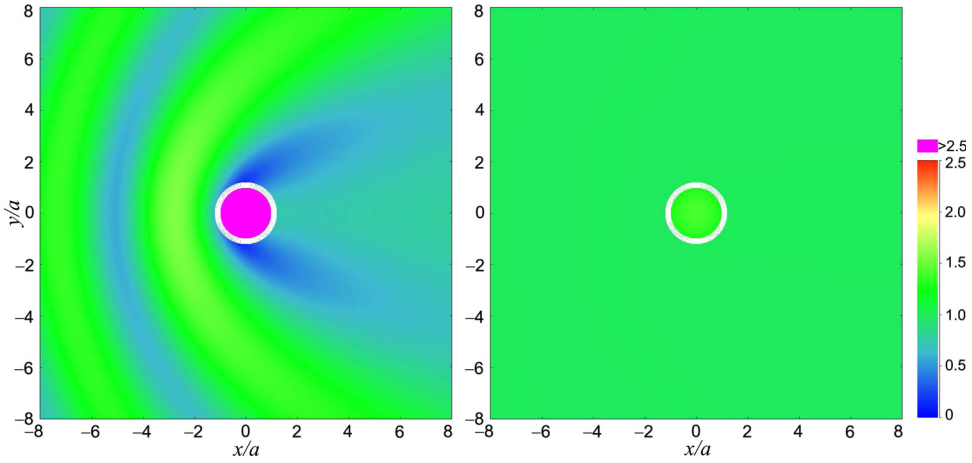

FIG. 11. (Color online) Distribution of amplitudes of total acoustic pressure when a planar incident wave of frequency $ka = 0.7$ impinges onto a cloaked resonating water column. The cloak is comprised of ten isotropic layers. Left: initial design. Right: cloak specifically optimized for cloaking at the resonant frequency.

cloaks based on the Cummer–Schurig prescription but using the isotropic equivalent layers have an additional level of frequency dependency: the isotropic-anisotropic equivalence is valid only at low frequencies. The frequency at which the optimization is run plays an extremely important role.

In the way the optimization is currently run, the objective is to reduce the total scattering cross section at one particular frequency, and whatever happen at other frequencies are totally disregarded. Yet, it has been repeatedly observed that the frequency at which the optimization is run determines the upper frequency limit of the cloaking effectiveness. The main reason for this is that these cloak designs are weakly frequency dependent. One frequency effectively represents all frequencies, until the frequency dependency becomes sufficiently strong.

For such weakly frequency-dependent cloaks, one example, in Sec. II A, shows that running the optimization at a frequency when the frequency dependency has become noticeable may actually extend the frequency range of the cloaking effectiveness. However, running the optimization at higher frequencies may also risk losing the cloaking effectiveness entirely. For example, in one attempt to optimize the ten-layer isotropic cloak at $ka = 6$, the normalized total scattering cross section at $ka = 6$ was reduced from 0.9 to 0.6, but it was increased from 0.05 to 2.0 and more in lower frequencies.

When cloaking strongly frequency dependent objects, the situation is different. Cloaking penetrable objects falls in this category, as even the Cummer–Schurig cloak becomes frequency-dependent.[12] For such cloaks, some compromises maybe needed, and Figs. 6 and 8 and Fig. 9 suggest a way to select the optimization frequency, depending on the desired outcome. If the suppressing a strong resonance is important, the cloak can be optimized to confine the resonance within the cloaked region. If, on the other hand, the primary goal is to have a wider frequency range in which cloaking is effective, the optimization can be run at those frequencies.

The current study has been focused on the possibilities the optimization may bring, and more importantly, on the question of whether the material singularity is a necessary condition for perfect cloaking. Although various optimization schemes have been implemented and used, the relative merits of one scheme over another have not been studied. However, the computations performed in this study show that different optimization runs, with different parameters or different schemes, lead to different parameter sets when they converge. The differences in general are not significant, but are not negligible, either. In other words, the optimization does not converge to the same solution. For this reason, throughout this paper, the outcome of an optimization run is called an optimized design, instead of an "optimal design." Another case to the point is when optimizing the cloak specifically for cloaking a water column. Intuitively, the "optimal" material choice for the cloak is water, because it will produce zero scattering cross section at any frequency. Interestingly enough, none of the optimization runs has reached that obvious "optimal design." This suggests that all the optimized designs obtained so far, in fact, in optimization terminology, are local minima.

VI. CONCLUSIONS

In this paper, gradient-based optimization schemes are used to fine tune the material properties of cloak designs based on the Cummer–Schurig cloaking prescription. It is demonstrated that, without material singularity and with a limit number of layers, the optimization is capable of reducing the normalized total scattering cross section to 0.002 or lower, a level that can be justifiably called perfect cloaking. In other words, material singularity is not a requirement for perfect cloaking. The removal of material singularity requirement would make the road to physical realization of perfect cloaking slightly easier, although other significant challenges remain. The price to pay for this advantage is that such a perfect cloaking is effective only within a limited, but still broad-band, frequency range.

Numerical examples also demonstrate that cloaks optimized for rigid objects also performed better than the initially design, when the cloaked object is changed. The optimization is even capable of suppressing a strongly resonant penetrable object at its resonance frequency, to completely confine the resonance to within the cloaked region, although at a cost of losing cloaking capability in most other frequencies. These examples demonstrate that, even if perfect cloaking is not the ultimate goal, optimization has great potential in many practical applications such as minimizing the target strength with given constraints in materials.

ACKNOWLEDGMENT

This work was supported by the Office of Naval Research (ONR) under Grant No. N000140910546. The author would like to thank Ms. Chunyan Bao for assistance in computations.

[1]D. Schurig, J. J. Mock, B. J. Justice, S. A. Cummer, J. B. Pendry, A. F. Starr, and D. R. Smith, "Metamaterial electromagnetic cloak at microwave frequencies," Science **314**, 977 (2006).
[2]J. B. Pendry, D. Schurig, and D. R. Smith, "Controlling electromagnetic fields," Science **312**, 1780–1782 (2006).
[3]U. Leonhardt, "Optical conformal mapping," Science **312**, 1777–1780 (2006).
[4]S. A. Cummer and D. Schurig, "One path to acoustic cloaking," New J. Phys. **9**, 45 (2007).
[5]Y. Cheng, F. Yang, J. Y. Xu, and J. L. Xiao, "A multilayer structured acoustic cloak with homogeneous isotropic materials," Appl. Phys. Lett. **92**, 151913 (2008).
[6]D. Torrent and J. Sánchez-Dehesa, "Acoustic cloaking in two dimensions: A feasible approach," New J. Phys. **10**, 063015 (2008).
[7]L.-W. Cai and J. Sánchez-Dehesa, "Analysis of equivalent anisotropy arising from dual isotropic layers of acoustic media," J. Acoust. Soc. Am., in press (2012).
[8]J. Hu, X. M. Zhou, and G. K. Hu, "Nonsingular two-dimensional cloak of arbitrary shape," Appl. Phys. Lett. **95**, 011107 (2009).
[9]L.-W. Cai, "Multiple scattering in single scatterers," J. Acoust. Soc. Am. **115**, 986–995 (2004).
[10]L.-W. Cai and J. Sánchez-Dehesa, "Acoustical scattering by radially stratified scatterers," J. Acoust. Soc. Am. **124**, 2715–2726 (2008).
[11]L.-W. Cai, D. K. Dacol, G. J. Orris, D. C. Calvo, and M. Nicholas, "Acoustical scattering by multilayer elastic scatterer containing electrorheological fluid layer," J. Acoust. Soc. Am. **129**, 12–23 (2011).
[12]L.-W. Cai and J. Sánchez-Dehesa, "Analysis of Cummer-Schurig acoustic cloaking," New J. Phys. **9**, 450 (2007).
[13]E. M. Hendrix and B. G.-Tóth, *Introduction to Nonlinear and Global Optimization* (Springer, New York, 2010), pp. 109–110.
[14]W. H. Press, S. A. Teukolsky, W. T. Vetterling, and B. P. Flannery, *Numerical Recipes*, 3rd ed. (Cambridge University Press, Cambridge, 2007), p. 496.